

# Delaying transition in Taylor-Couette flow with axial motion of the inner cylinder

By AREL Y. WEISBERG<sup>†</sup>, IOANNIS G. KEVREKIDIS<sup>‡</sup>  
AND ALEXANDER J. SMITS

Department of Mechanical and Aerospace Engineering  
Princeton University  
Princeton, New Jersey 08544-0710, U.S.A.

(Received 12 March 1997)

Periodic axial motion of the inner cylinder in Taylor-Couette flow is used to delay transition to Taylor vortices. The outer cylinder is fixed. The marginal stability diagram of Taylor-Couette flow with simultaneous periodic axial motion of the inner cylinder is determined using flow visualization. For the range of parameters studied, the degree of enhanced stability is found to be greater than that predicted by Hu & Kelly (1995), and differences in the scaling with axial Reynolds number are found. The discrepancies are attributed to essential differences between the base flow in the open system considered by Hu & Kelly, where mass is conserved over one period of oscillation, and the base flow in the enclosed experimental apparatus, where mass is conserved at all sections at all times.

---

## 1. Introduction

The central importance of flow between concentric cylinders as a fluid-dynamical paradigm has been well documented in the reviews by Di Prima & Swinney (1985) and Tagg (1994). One reason for the great number of studies of this “Taylor-Couette” flow is the orderly progression of nonlinear flow states observed in the system as it undergoes transition to turbulence. For example, if the outer cylinder is held fixed and the inner one rotates at angular speed  $\Omega$ , a series of four critical speeds exist between the purely azimuthal Couette flow at low values of  $\Omega$  and the turbulent Taylor vortices that appear at large values of  $\Omega$  (Andereck *et al.*, 1986). This orderly progression to turbulence makes Taylor-Couette flow attractive as a model for studying transition to turbulence in more complex systems.

The first transition, from steady azimuthal flow to Taylor vortices, has been the focus of many previous studies. Variations of the basic Taylor-Couette flow experiment which raise the critical angular speed for this transition have also been explored. In particular, Taylor-Couette flow with superposed Poiseuille flow (that is, a non-zero axial through-flow) has been studied experimentally by Cornish (1933), Fage (1938), Kaye & Elgar (1957), Donnelly & Fultz (1960), Snyder (1962), Schwartz *et al.* (1964), Takeuchi & Jankowski (1981), Buhler & Polifke (1990), Babcock *et al.* (1991), Lueptow *et al.* (1992), Tsameret & Steinberg (1994) and Tsameret *et al.* (1994), and analytically by Goldstein (1937), Chandrasekhar (1960), Di Prima (1960), Krueger & Di Prima (1964), Chung

<sup>†</sup> Present address: SciTec, Inc., 100 Wall St., Princeton NJ 08540

<sup>‡</sup> Department of Chemical Engineering

& Astill (1977), Takeuchi & Jankowski (1981), Buhler & Polifke (1990), Tsameret & Steinberg (1994) and Tsameret *et al.* (1994). These efforts established that the critical rotation rate increases with increasing axial flow rates.

Taylor-Couette flow with superposed axial Couette flow (that is, where one of the cylinders is moving in the axial direction) has also been studied analytically (Ludweig, 1960, Kiessling, 1963, Wedemeyer, 1967) and experimentally (Ludweig, 1964) but much less extensively than the axial Poiseuille flow case. In all these studies both cylinders were rotating. In addition, a number of researchers examined the general case of both axial Couette and axial Poiseuille flow (Joseph & Munson, 1970, Hung *et al.*, 1972), including a numerical linear stability analysis for a finite flow domain (Ali & Weidman, 1993).

All the previously mentioned investigations were confined to steady axial flows. However, Hu & Kelly (1995) performed a linear stability analysis to include the effects of periodically varying axial pressure gradients and inner cylinder axial speeds, for the case of the inner cylinder rotating, as well as for the cases where the cylinders were co-rotating and counter-rotating. For periodic axial motion of the inner cylinder, with only the inner cylinder rotating, Hu & Kelly found enhanced stability for all axial speeds and oscillation frequencies. In the case of an open flow, corresponding to infinitely long cylinders, the fluid pathlines at subcritical angular speeds consist of constant radius spirals that ascend and descend in response to the inner cylinder's axial motion. Here, the azimuthal and axial velocity profiles are decoupled, so changes in the axial motion have no effect on the azimuthal velocity field. Once the flow undergoes transition to Taylor vortices the flow field becomes much more complex, but it still instantaneously resembles closely the Taylor-vortex-dominated flow-field which exists when axial motion is not present. This observation, coupled with the fact that the axial and azimuthal subcritical flow fields are independent, yield the supposition that the stability of Taylor-Couette flow with axial motion of the inner cylinder is closely related to the stability of Taylor-Couette flow *without* axial motion of the inner cylinder.

## 2. Experiment

To study these questions further, the experimental apparatus depicted in Figure 1 was constructed. Angular motion of the inner cylinder is controlled by a stepper motor, through a timing belt drive and a splined shaft. This shaft fits in a splined bushing in the top end cap, which, together with the ball joint in the bottom end cap, enabled the inner cylinder to be simultaneously spun as well as translated in the axial direction. The axial motion was controlled by a separate stepper motor through a variable ratio timing belt drive and a Scotch yoke mechanism, which imparts a sinusoidally varying axial velocity to the inner cylinder. The dimensions of the apparatus are shown in Table 1 and Figure 1. The top and bottom seals are rigidly attached to the outer cylinder, and are therefore non-rotating. The inner edges of the seals were machined to knife edges but they could not provide perfect dynamic seals, and therefore an overflow reservoir was designed into the top seal, and a second, spring-loaded, rubber lip seal (not shown) was incorporated into the base cylinder.

The working fluid used throughout this work was a 20:1 mixture of distilled water and Kalliroscope AQ-1000 rheoscopic concentrate<sup>†</sup>. The flakes align themselves with the local shear stress direction thereby making flow patterns visible. When the “face” of a flake is oriented toward the observer incident light is reflected back, “coloring” the

<sup>†</sup> Kalliroscope Corporation, 264 Main St., Box 60, Groton MA 01450, (508) 448-6302

local fluid white. When the flake is oriented sideways light is not reflected back to the observer, and the fluid appears darker. These flakes have been used in many previous Taylor-Couette flow experiments (Andereck *et al.*, 1986). When using the water and Kalliroscope mixture, the flow field appears to be uniformly gray at subcritical angular speeds. Once Taylor vortices ( which are pairs of counter-rotating toroidal vortices) appear, the flow field displays alternating light and dark bands indicating the presence of vortices of opposite sign.

The kinematic viscosity of the mixture as a function of temperature was measured to within 1% by a professional laboratory. The apparatus was placed in a temperature controlled enclosure, resulting in a temperature fluctuation of less than 0.2°C. The uncertainty in the value of the kinematic viscosity due to temperature and other sources of error is less than 1.4%. Settling of the Kalliroscope flakes can introduce a viscosity gradient, but under our experimental conditions the uncertainty in the viscosity was dominated by temperature variations. When the cylinders are vertical, as in the current experiment, the slowly increasing Kalliroscope flake concentration is known to affect slightly the wavelength of the Taylor vortices (Dominguez-Lerma *et al.*, 1985), but the effect on the critical Taylor number is not known. This issue is addressed further below.

The onset of transition to Taylor vortices was recorded by a black and white CCD video camera connected to a personal computer which acquired and stored the images directly. The images were processed using a modified version of the public domain image processing program NIH Image† for the Macintosh. Custom stepper motor control circuitry was built which enabled both stepper motors in the experiment to be completely controlled by software (for further details of the image processing procedure and the electronic control circuitry, see Weisberg, 1996).

Three dimensionless parameters determine the state of the system. Following Hu & Kelly, we use a Taylor number,  $Ta$ , based on the rotation rate of the inner cylinder, a Reynolds number,  $Re$ , based on the maximum axial speed of the inner cylinder, and an oscillation parameter,  $\beta$ , where the axial frequency of oscillation was non-dimensionalized by the viscous time scale:

$$Ta = \frac{4\Omega^2\eta^2d^4}{(1-\eta^2)\nu^2}, \quad Re = \frac{U_{max}d}{\nu}, \quad \beta = \sqrt{\frac{\omega d^2}{2\nu}},$$

where  $\Omega$  is the angular speed of the inner cylinder,  $\eta$  is the radius ratio  $r_i/r_o$  of the cylinders ( $= 0.9051$ ),  $d$  is the gap size ( $= r_o - r_i$ ),  $\nu$  is the kinematic viscosity of the working fluid,  $U_{max}$  is the amplitude of axial speed of the inner cylinder, and  $\omega$  is the (angular) frequency of the axial motion of the inner cylinder. The experimental uncertainties are:  $\delta Ta = 3.1\%$ ,  $\delta Re = 2.1\%$ , and  $\delta\beta = 0.71\%$ .

### 3. Results

To determine the critical value of the Taylor number as a function of Reynolds number and the oscillation parameter, the rotation rate of the inner cylinder was increased very slowly and the flow field was monitored for the presence of Taylor vortices. A number of experiments were conducted to determine quasi-static levels of acceleration, and to determine the threshold at which it was judged that transition had occurred. In most experimental systems, Taylor vortices first appear near the ends of the cylinders at lower

† NIH Image developed at the U.S. National Institutes of Health and available from the Internet by anonymous FTP from [zippy.nimh.nih.gov](http://zippy.nimh.nih.gov) or on floppy disk from the National Technical Information Service, Springfield, Virginia, part number PB95-500195GEI

than expected values of  $Ta$ . The extent of the flow domain dominated by Taylor vortices then spreads from the end walls toward the center of the apparatus, until, for systems with large aspect ratios (cylinder length/gap width), the vortices meet at mid-length at what we expect to correspond to the theoretical critical value of the Taylor number (Lueptow *et al.*, 1992). In contrast to previous experimental work, the vortices observed in this experiment appeared at the lower end first, and propagated up towards the center at progressively higher values of  $Ta$ . This sequence is shown in Figure 2. The reason for this discrepancy is not clear. There exists a slight eccentricity of the cylinders at the top of the flow domain but the level of eccentricity (a maximum of 0.005 *in*, or 0.6% of the gap size) is a factor of 5 less than the level at which the critical Taylor number begins to be reduced (Cole, 1976). For our experiment, transition to Taylor vortices was defined as the value of  $Ta$  at which the vortices reached the center of the cylinders. This definition yielded consistent values for the critical Taylor number in a variety of experiments in which the initial speed and the acceleration rate of the inner cylinder was varied. The effects of gravity on the Kalliroscope concentration also seems to be rather small, given the typical duration of an experiment was very much less than the settling time of the flakes.

In fact, using this definition, the critical Taylor number,  $Ta_{c,0}$ , for ordinary Taylor-Couette flow ( $Re = 0$ ) was determined to be  $= 3636 \pm 3.6\%$ . This value compares very well with the values found by previous experimental and analytical studies, as indicated in Figure 3. The same method used to obtain  $Ta_{c,0}$  was used to determine  $Ta_c$ , the transitional value of  $Ta$  at nonzero  $Re$  and  $\beta$ . Note that, for our apparatus,  $Re$  and  $\beta$  were not independent, and  $Re \propto \beta^2$ .

The results for  $Ta_{c,0}$  are shown in Figure 4. Two axial drive reduction ratios were used to obtain the two sets of data for  $Re = 6.35\beta^2$ . The agreement between these two sets demonstrates that the results are independent of the particular experimental configuration. Very recently, Marques & Lopez (1996) by a numerical linear stability analysis determined the critical Taylor numbers for the case of an enclosed system similar to that studied in the experiment. The agreement between their results and the experimental data is extremely good, as seen in Figure 4.

Hu & Kelly found that the increase in the critical Taylor number scales with  $Re^2$  for  $Re < 30$ , and their results for  $Re = 1$  and  $Re \ll 1$  very nearly coincide with the results for  $Re = 30$  for the range of  $\beta$  examined here ( $0 \leq \beta \leq 10$ ). The data in Figure 4, for  $Re$  ranging from approximately 10 to 100, was therefore rescaled with  $Re^2$  and replotted in Figure 5.

A number of preliminary conclusions can be drawn from Figure 5. The experimental data and analytical results converge at the larger values of the oscillation parameter  $\beta$ . This is expected, since as the axial frequency is increased, the effects of the oscillating inner cylinder will propagate shorter and shorter distances into the gap due to the damping effects of viscosity. Therefore in the limit of very large values of  $\beta$ , the data and analytical results should approach the critical value of  $Ta$  corresponding to  $Re = 0$ .

For values of  $\beta$  greater than approximately 1.5, the  $Re^2$  scaling is broadly evident in the data although the experimental data and analytical results do not agree. At values of  $\beta$  below 1.5, the  $Re^2$  scaling is less evident, and the trends in the experimental data and analytical results differ as well. While Hu & Kelly's results are nearly constant for  $\beta < 1$  in the scaling of Figure 5, the experimental data points appear to be increasing with diminishing  $\beta$ . The loss of scaling with  $Re^2$  is most likely due to the higher values of  $Re$  associated with many of the data points.

While Hu & Kelly computed results for  $Re = 30$ , the largest value of  $Re$  in the data is close to 100. Further, with the breakdown of the  $Re^2$  scaling, the uncertainty

envelope grows. The growth of the uncertainty in the data, as scaled in Figure 5, is also substantially larger than that seen in Figure 4 due to the presence of the  $1/Re^2$  term. However, the ratio of parameters on the vertical axis greatly magnifies the experimental uncertainties in the parameters  $Ta_c$ ,  $Ta_{c,0}$  and  $Re$ , and therefore it misrepresents the high degree of accuracy in the measurements. The behavior of the experimental results is more satisfactorily demonstrated in the form given in Figure 4.

Outside the range of  $Re$  and  $\beta$  values shown in Figure 4 there are values of  $Re$  and  $\beta$  at which a different transition was observed to take place. In these cases vortices did not propagate in an orderly fashion from the bottom end of the apparatus, but appeared in various locations intermittently. At larger values of  $Ta$  the vortices became increasingly permanent until they filled the apparatus at all times. These vortices were often tilted with respect to the axis of rotation. Because of the different nature of this transition, those results are not shown here, although they present an interesting direction in which to extend this investigation.

#### 4. Discussion and Conclusions

We propose that the discrepancies between the analytical results presented by Hu & Kelly (1995) and the experimental data given here are due to the fundamental differences in the subcritical flow fields (the “base” flows): the experiment was an “enclosed” system, whereas Hu & Kelly considered an “open” system. In an open flow system, mass is conserved over an entire axial period through any cross section normal to the axis of rotation. In an enclosed system, however, net mass flux through any cross section is zero at all times. At low values of  $\beta$  the base flow in open systems is unidirectional over most of the axial period. In contrast, the base flow in an enclosed system will always consist of equal fluid volumes travelling in opposite directions.

As  $\beta$  is increased from zero, the base flow in the open system develops regions of reversed flow. This can be seen as the growth of the viscous time scale,  $d^2/\nu$ , relative to the axial period. Consequently, in the range of  $\beta$  between approximately 2 and 4, the two types of base flows more closely resemble one another. At larger values of  $\beta$  the axial base flow is almost stationary except close to the inner cylinder wall because viscosity damps out the axial oscillations well before they can propagate into the gap. This is true of the base flow in both the open and enclosed cases.

These differences help to explain why the experimental data and analytical results approach one another at larger values of  $\beta$  and diverge at lower values. Additional insight can be acquired using just the trend in Hu & Kelly’s results. In particular, the magnitude of azimuthal vorticity in the base flow field, which arises as a consequence of the axial motion, appears to play a key role. At values of  $\beta < 1$  the axial velocity profile in the open system, which is nearly linear in the case of  $\eta \approx 1$ , has very little curvature, and therefore the azimuthal component of the vorticity field is determined by the slope of the axial velocity profile. As  $\beta$  increases, the axial velocity develops regions of reversed flow, and the magnitude of the azimuthal vorticity in the flow, integrated over the gap size, increases. This results in increased stability enhancement when normalized by  $Re^2$ , as the analytical results in Figure 5 indicate. As  $\beta$  increases further, viscous damping reduces the magnitude of the vorticity in the flow, and the degree of enhanced stability reduces as well.

The role of azimuthal vorticity becomes clearer when the vorticity distribution in supercritical Taylor-Couette flow with  $Re = 0$  is considered. When the flow field is dominated by Taylor vortices, the azimuthal vorticity changes sign along the axial direction. Consequently, transition from subcritical flow to supercritical flow can be viewed

as the generation of azimuthal vorticity, with equal amounts of fluid acquiring either positive or negative azimuthal vorticity. However, when  $Re > 0$  the fluid already contains azimuthal vorticity that is a function of radial position only. Therefore, transition to Taylor vortices, which have axial variations in azimuthal vorticity, will require that some of the fluid's azimuthal vorticity undergo a sign reversal. To undergo this change, it is likely that higher than usual values of  $Ta$  will be required to reverse the local angular momentum vectors to this extent, which indicates a flow that is centrifugally unstable to a greater degree. For the case of steadily translating cylinders ( $\beta = 0$ ) the predicted change in  $Ta$  can be readily calculated:

$$\Delta Ta_{encl} \propto \frac{1}{r_0 - r_i} \int_{r_i}^{r_0} \omega_{\theta, encl}^2 r dr$$

$$\Delta Ta_{\infty} \propto \frac{1}{r_0 - r_i} \int_{r_i}^{r_0} \omega_{\theta, \infty}^2 r dr$$

where  $\omega_{\theta}$  is the azimuthal vorticity,  $\Delta Ta = Ta_c - Ta_{c,0}$ , and the subscripts  $\infty$  and *encl* denote the open and enclosed systems, respectively. Inserting the expressions for the azimuthal vorticity for each case we find that:

$$\frac{\Delta Ta_{encl}}{\Delta Ta_{\infty}} = \frac{\int_{r_i}^{r_0} \omega_{\theta, encl}^2 r dr}{\int_{r_i}^{r_0} \omega_{\theta, \infty}^2 r dr} = 3.8$$

After accounting for the lower value of  $\eta$  in the experiments versus the calculations, this value should be 3.5. This number is in good agreement with the experimental data: extrapolating the data in Figure 5 to  $\beta = 0$  gives a value of this ratio of about 3 (3.5 falls within the experimental uncertainty). The increased level of the azimuthal vorticity therefore seems to be a good indication of the enhanced stability of the system.

These considerations were first presented by Weisberg (1996). The numerical linear stability analysis by Marques & Lopez (1996) agrees extremely well with the experiment (see Figure 4), providing strong analytical support for the physical arguments presented here and by Weisberg (1996). The divergent trend seen at low  $\beta$  in Figure 5 was also reproduced in their enclosed flow analysis, as was the breakdown of the  $Re^2$  scaling for values of  $Re > 30$ .

In summary, the marginal stability curve for Taylor-Couette flow has been determined experimentally for the range of parameters:  $0.5 < \beta < 6.0$ ,  $10 < Re < 100$ . The curve traced by the experimental values was found to lie above the curve calculated by Hu & Kelly. It was suggested that this occurs because, in contrast to the system considered by Hu & Kelly, the experiment was an enclosed flow system. Given the essential differences in the subcritical flow fields, as well as the trends in Hu & Kelly's results, it appears that the integral of the square of azimuthal vorticity over the gap plays an important role in the degree of enhanced stability. The greater the square of the azimuthal vorticity, the greater is the enhanced stability. A physical argument can be made that this enhanced stability results because transition from Taylor-Couette flow with axial motion of the inner cylinder requires a greater change in the azimuthal vorticity of the fluid than in the case without axial motion.

This work was partially supported by: The Guggenheim Fellowship fund, AFOSR

(Grant numbers F49620-93-1-0427, F49620-93-1-0478, F49620-93-1-0476), DARPA Grants N00014-92-J-1796 and N00014-91-J-1850, NSF Grants CTS-89-57213 and ECS- 90-23362, and ONR/ARPA AASERT proposal N00014-94-1-0149.

## References

- Ali, M.E. & Weidman, P.D. 1993. On the linear stability of cellular spiral Couette flow. *Physics of Fluids A*, **5**(11), 1188–1200.
- Andereck, C.D., Liu, S.S. & Swinney, H.L. 1986. Flow regimes in a circular Couette system with independently rotating cylinders. *Journal of Fluid Mechanics*, **164**, 155–183.
- Babcock, K.L., Ahlers, G. & Cannell, D.S. 1991. Noise-sustained structure in Taylor-Couette flow with through flow. *Physical Review Letters*, **67**(24), 3388.
- Buhler, K. & Polifke, N. 1990. Dynamical behavior of Taylor vortices with superimposed axial flow. *Pages 21–29 of: Busse, F.H. & Kramer, L. (eds), Nonlinear Evolution of Spatio-Temporal Structures in Dissipative Continuous Systems*. Plenum Press, New York.
- Chandrasekhar, S. 1960. The hydrodynamic stability of viscous flow between coaxial cylinders. *Pages 141–143 of: Proceedings of the National Academy of Science, U.S.A.*, vol. 46.
- Chung, K.C. & Astill, K.N. 1977. Hydrodynamic instability of viscous flow between rotating coaxial cylinders with fully developed axial flow. *Journal of Fluid Mechanics*, **81**, 641–655.
- Cole, J.A. 1976. Taylor-vortex instability and annulus-length effects. *Journal of Fluid Mechanics*, **75**, 1–15.
- Cornish, R.J. 1933. Flow of water through fine clearances with relative motion of the boundaries. *Proc. Roy. Soc. Lond. A*, **140**, 227–240.
- Di Prima, R.C. 1960. The stability of a viscous fluid between rotating cylinders with an axial flow. *Journal of Fluid Mechanics*, **9**, 621–631.
- Di Prima, R.C. & Swinney, H.L. 1985. Instabilities and transition in flow between concentric rotating cylinders. *Pages 139–180 of: Swinney, H.L. & Gollub, J.P. (eds), Hydrodynamic Instabilities and the Transition to Turbulence*, 2 edn. Topics in Applied Physics, vol. 45. Springer-Verlag, Berlin.
- Dominguez-Lerma, M.A., Ahlers, G. & Cannell, D.S. 1985. Effects of “Kalliroscope” flow visualization particles on rotating Couette-Taylor flow. *Physics of Fluids*, **24**(4), 1204–1206.
- Donnelly, R.J. & Fultz, D. 1960. Experiments on the stability of spiral flow between rotating cylinders. *Pages 1150–1154 of: Proceedings of the National Academy of Sciences, U.S.A.*, vol. 46.
- Fage, E. 1938. The influence of wall oscillations, wall rotation, and entry eddies on the breakdown of laminar flow in an annular pipe. *Proc. Roy. Soc. Lond. A*, **165**, 513–517.
- Goldstein, S. 1937. The stability of viscous fluid flow between rotating cylinders. *Proceedings of the Cambridge Philosophical Society*, **33**, 41–61.
- Hu, H.-C. & Kelly, R. 1995. Effect of a time-periodic axial shear flow upon the onset of Taylor vortices. *Physical Review E*, **51**(4), 3242–3251.
- Hung, W.L., Joseph, D.D. & Munson, B.R. 1972. Global stability of spiral flow. Part 2. *Journal of Fluid Mechanics*, **51**, 593–612.
- Joseph, D.D. & Munson, B.R. 1970. Global stability of spiral flow. *Journal of Fluid Mechanics*, **43**, 545–575.

- Kaye, J. & Elgar, E.C. 1957. Modes of adiabatic and diabatic fluid flow in an annulus with an inner rotating cylinder. *Transactions of the ASME*, **80**, 753–765.
- Kiessling, I. 1963. Characteristics of turbulence in a boundary layer with zero pressure gradient. *Deutsche Versuchsanstalt für Luft und Raumfahrt, Bericht 290*.
- Krueger, E.R. & Di Prima, R.C. 1964. The stability of a viscous fluid between rotating cylinders with an axial flow. *Journal of Fluid Mechanics*, **19**, 528–538.
- Ludweig, H. 1960. Stabilität der Strömung in einem zylindrischen Ringraum. *Zeitschrift für Flugwissenschaften*, **8**, 135.
- Ludweig, H. 1964. Experimentelle Nachprüfung der Stabilitätstheorien für reibungsfreie Strömungen mit schraubenlinienförmigen Strömlinien. *Zeitschrift für Flugwissenschaften*, **12**, 304–309.
- Lueptow, R.M., Docter, A. & Kyungyoon, M. 1992. Stability of axial flow in an annulus with a rotating inner cylinder. *Physics of Fluids A*, **4**(11), 2446–2455.
- Marques, F. & Lopez, J.M. 1996. Taylor-Couette flow with axial oscillations of the inner cylinder: Floquet analysis of the basic flow. *Submitted for publication, J. Fluid Mech.*
- Schwartz, K.W., Springett, B.E. & Donnelly, R.J. 1964. Modes of instability in spiral flow between rotating cylinders. *Journal of Fluid Mechanics*, **20**, 281–289.
- Snyder, H.A. 1962. Experiments on the stability of spiral flow at low axial Reynolds numbers. *Proc. Roy. Soc. Lond. A*, **265**, 198–214.
- Tagg, R. 1994. The Couette-Taylor problem. *Nonlinear Science Today*, **4**(3), 1–25.
- Takeuchi, D.I. & Jankowski, D.F. 1981. A numerical and experimental investigation of the stability of spiral Poiseuille flow. *Journal of Fluid Mechanics*, **102**, 101–126.
- Tsameret, A. & Steinberg, V. 1994. Absolute and convective instabilities and noise-sustained structures in the Couette-Taylor system with an axial flow. *Physical Review E*, **49**(2), 1291–1308.
- Tsameret, A., Goldner, G. & Steinberg, V. 1994. Experimental evaluation of the intrinsic noise in the Couette-Taylor system with an axial flow. *Physical Review E*, **49**(2), 1309–1319.
- Wedemeyer, E. 1967. Einfluss der Zähigkeit auf die Stabilität der Strömung in einem schmalen Ringraum mit zusätzlichem, axialem Durchfluss. *AVA-Bericht 67*, **A34**.
- Weisberg, A.Y. 1996. *Control of transition in Taylor-Couette flow with axial motion of the inner cylinder*. Ph.D. Thesis, Princeton University.

## Tables and Figures

Table 1. Summary of cylinder dimensions.

Figure 1. Schematic drawing of the apparatus. All dimensions are in inches.

Figure 2. From top to bottom, Taylor vortices propagating into the flow domain at subcritical ( $0.85 Ta_{c,0}$ ), critical and supercritical ( $1.1 Ta_{c,0}$ ) values of the Taylor number  $Ta$ .

Figure 3. Critical values of the Taylor number in ordinary Taylor-Couette flow ( $Re = 0$ ),  $Ta_{c,0}$  as a function of the radius ratio,  $\eta$ .  $\diamond$ , present results. The other experimental ( $\times$ ) and theoretical ( $\circ$ ) values are taken from Lueptow *et al.* (1992) and Cole (1976), and their cited sources. The theoretical values are shown with their best linear curve fit.

Figure 4. Enhanced stability of Taylor-Couette flow with axial motion of the inner cylinder as a function of  $Re$  and  $\beta$ . Experiments:  $\circ$ ,  $Re = 1.59\beta^2$ ;  $\square$ ,  $Re = 3.18\beta^2$ ;  $\diamond$ ,  $Re = 6.35\beta^2$ ;  $\triangle$ ,  $Re = 6.35\beta^2$  (in a different experimental configuration);  $\circ$ ,  $Re = 12.7\beta^2$ ;  $\square$ ,  $Re = 25.6\beta^2$ ;  $\diamond$ ,  $Re = 41.3\beta^2$ . The uncertainty in each measurement is between 3% and 4%. The solid lines are the results of the analysis by Marques & Lopez (1996).

Figure 5. Enhanced stability due to axial motion of the inner cylinder normalized by  $Re^2$  as a function of the oscillation parameter  $\beta$ . Symbols are as given in Figure 4. The range of uncertainty in the measurements is given by the distance between the solid lines. The analytical results by Hu & Kelly (1995) for  $Re = 30$  and  $\beta \leq 6$  are indicated by the  $\times$  symbol.

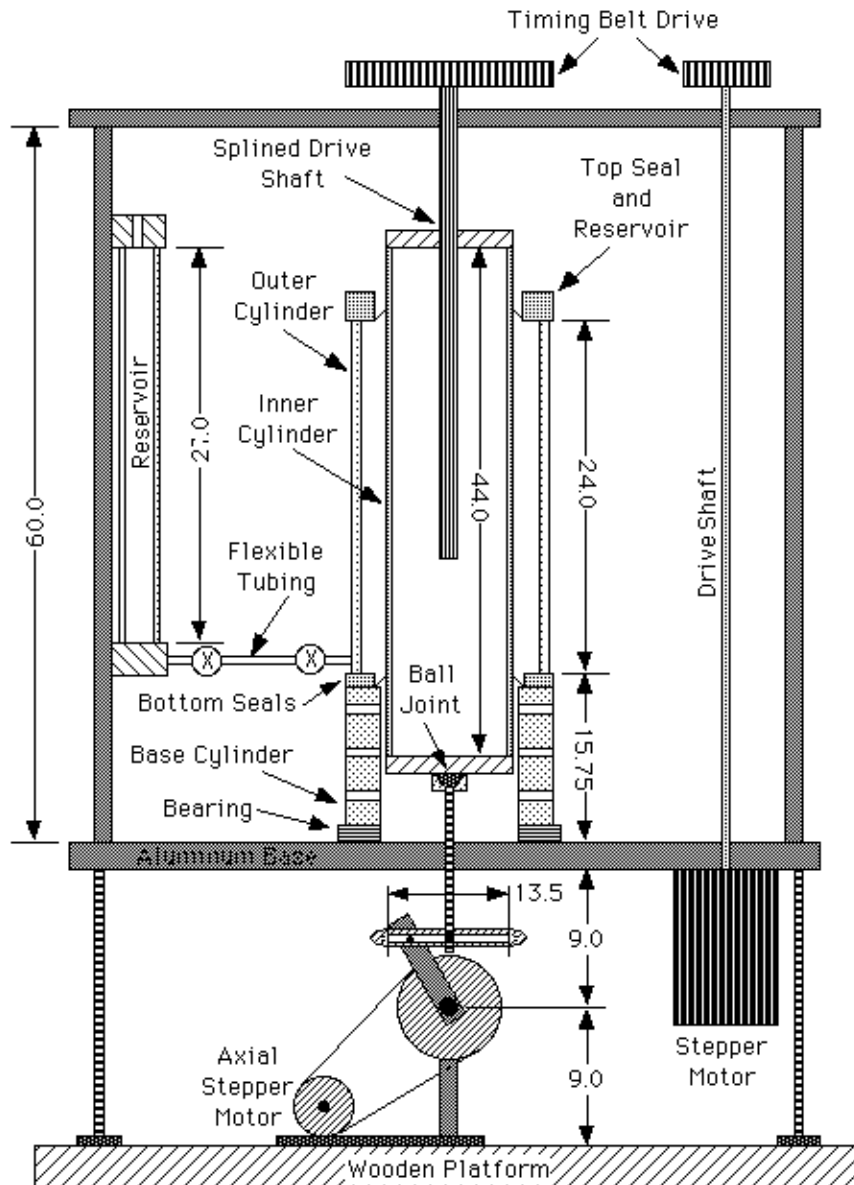


FIGURE 1. Schematic drawing of the apparatus. All dimensions are in inches.



FIGURE 2. From top to bottom, Taylor vortices propagating into the flow domain at subcritical ( $0.85 Ta_{c,0}$ ), critical and supercritical ( $1.1 Ta_{c,0}$ ) values of the Taylor number  $Ta$ .

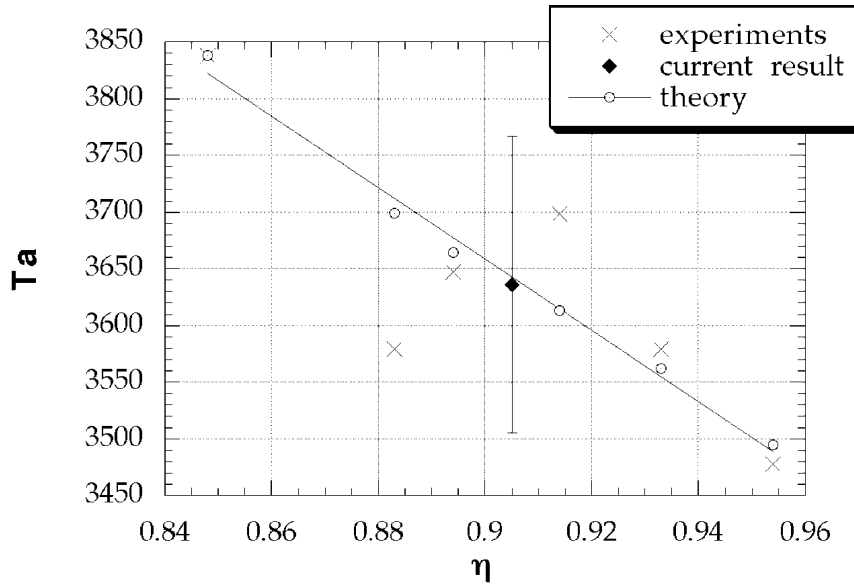


FIGURE 3. Critical values of the Taylor number in ordinary Taylor-Couette flow ( $Re = 0$ ),  $Ta_{c,0}$  as a function of the radius ratio,  $\eta$ .  $\diamond$ , present results. The other experimental ( $\times$ ) and theoretical ( $\circ$ ) values are taken from Lueptow *et al.* (1992) and Cole (1976), and their cited sources. The theoretical values are shown with their best linear curve fit.

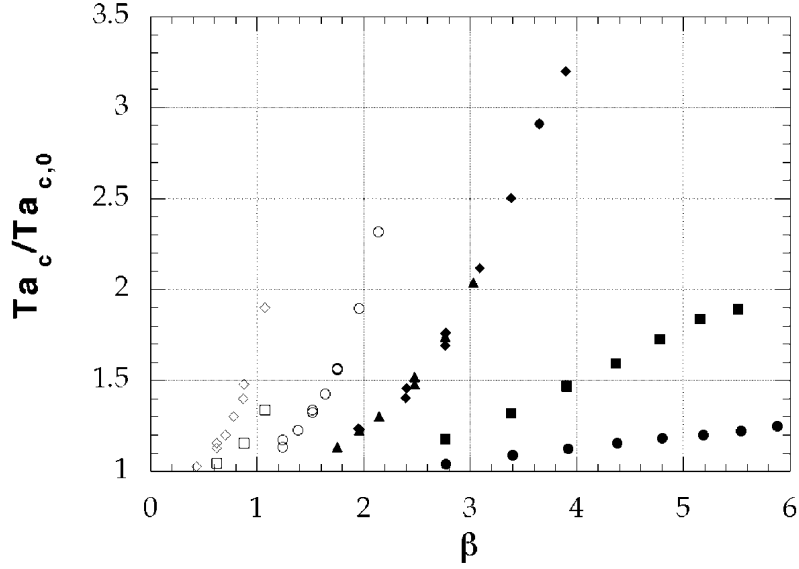


FIGURE 4. Enhanced stability of Taylor-Couette flow with axial motion of the inner cylinder as a function of  $Re$  and  $\beta$ . Experiments:  $\circ$ ,  $Re = 1.59\beta^2$ ;  $\square$ ,  $Re = 3.18\beta^2$ ;  $\diamond$ ,  $Re = 6.35\beta^2$ ;  $\triangle$ ,  $Re = 6.35\beta^2$  (in a different experimental configuration);  $\circ$ ,  $Re = 12.7\beta^2$ ;  $\square$ ,  $Re = 25.6\beta^2$ ;  $\diamond$ ,  $Re = 41.3\beta^2$ . The uncertainty in each measurement is between 3% and 4%. The solid lines are the results of the analysis by Marques & Lopez (1996).

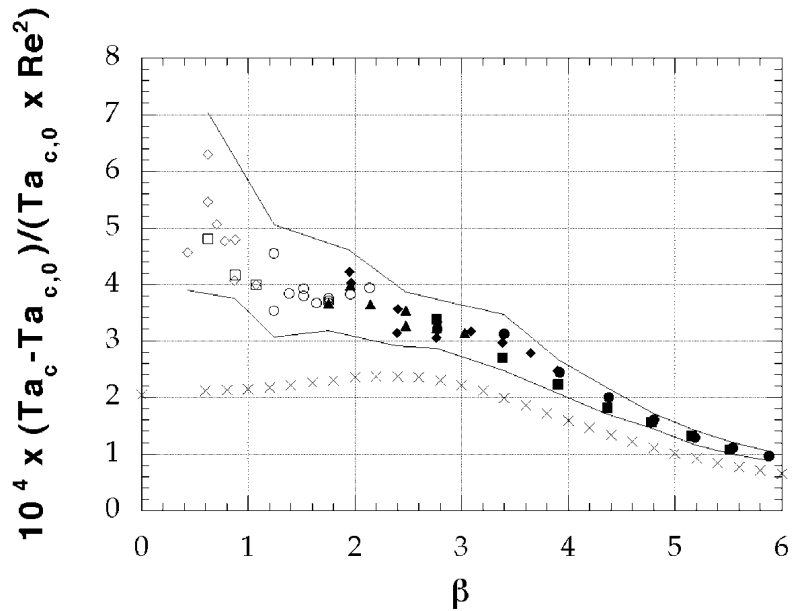


FIGURE 5. Enhanced stability due to axial motion of the inner cylinder normalized by  $Re^2$  as a function of the oscillation parameter  $\beta$ . Symbols are as given in Figure 4. The range of uncertainty in the measurements is given by the distance between the solid lines. The analytical results by Hu & Kelly (1995) for  $Re = 30$  and  $\beta \leq 6$  are indicated by the  $\times$  symbol..